JACS
JOURNAL OF THE AMERICAN CHEMICAL SOCIETY
pubs.acs.org/JACS
Communication

Daytime Atmospheric Halogen Cycling through Aqueous-Phase Oxygen Atom Chemistry

Evan Z. Dalton, Erik H. Hoffmann, Thomas Schaefer, Andreas Tilgner, Hartmut Herrmann, and Jonathan D. Raff*

Cite This: J. Am. Chem. Soc. 2023, 145, 15652−15657
Read Online
ACCESS | Metrics & More | Article Recommendations | Supporting Information

ABSTRACT: Halogen atoms are important atmospheric oxidants that have unidentified daytime sources from photochemical halide oxidation in sea salt aerosols. Here, we show that the photolysis of nitrate in aqueous chloride solutions generates nitryl chloride ($ClNO_2$) in addition to Cl_2 and HOCl. Experimental and modeling evidence suggests that $O(^3P)$ formed in the minor photolysis channel from nitrate oxidizes chloride to Cl_2 and HOCl, which reacts with nitrite to form $ClNO_2$. This chemistry is different than currently accepted mechanisms involving chloride oxidation by OH and could shift our understanding of daytime halogen cycling in the lower atmosphere.

Chlorine atoms are highly reactive oxidants that, besides their role in stratospheric chemistry, impact the lower atmosphere by oxidizing volatile organic compounds, converting marine reduced sulfur emissions into aerosol sulfate, and depleting ozone in the polar boundary layer.[1−4] Precursors of Cl include photolabile gases such as Cl_2, HOCl, $ClNO_2$, and ClNO released into the gas phase when oxidants such as OH, O_3, N_2O_5, and NO_2 react on or within sea salt aerosols (SSA).[5−9] Recent field studies document daytime $Cl_{2(g)}$ concentrations in the marine boundary layer (MBL) that are higher than levels predicted by models considering established sources, suggesting that a strong photochemical source is needed to balance photochemical loss.[10−14] Here we show that nitrate photolysis in the presence of $Cl^-_{(aq)}$ produces $ClNO_{2(g)}$ in addition to $Cl_{2(g)}$ and $HOCl_{(g)}$. Laboratory experiments and kinetic modeling show that oxidation of Cl^- to Cl_2 and HOCl occurs via ground-state oxygen atoms, $O(^3P)$, and the subsequent reaction of Cl_2 and HOCl with NO_2^- is responsible for the evolution of observed $ClNO_{2(g)}$. Not only is this an unrecognized source of active halogens in the lower atmosphere, but it also suggests that $O(^3P)$ plays an important role in aqueous-phase oxidation chemistry via a class of reactions that, until now, has not been adequately considered in kinetic and chemical transport models.

Nitrate is a common component of SSA due to reactions between halide ions and N_2O_5, HNO_3, and NO_2 in the polluted marine boundary layer, where NO_3^- concentrations in SSA can be ∼100−300 mM.[15] First suggested by Gori et al.[16] and demonstrated more recently in laboratory studies,[13,17−21] photolysis of NO_3^- oxidizes halides to photochemically active halogen species such as Br_2, Cl_2, and BrCl. The putative mechanism associated with active halogen formation involves the oxidation of halides by hydroxyl radicals (OH) stemming from the photodissociation of nitrate (reaction 1a).[22,23]

$$NO_3^- + H^+ + h\nu \rightarrow NO_2 + OH \quad (1a)$$

$$\rightarrow NO_2^- + O(^3P) \quad (1b)$$

A second photochemical channel forms nitrite (NO_2^-) and ground-state oxygen atoms, $O(^3P)$ (reaction 1b). The quantum yields of reactions 1a and 1b are 1.7%[23] and 1%,[24] respectively, at 298 K and wavelengths above 300 nm, although actual quantum yields remain uncertain.[24,25] Previous work has shown that OH reacts with Cl^- via an acid-assisted mechanism, forming Cl_2 according to reactions 2−5:[26]

$$OH + Cl^- \rightleftharpoons HOCl^- \quad (2)$$

$$HOCl^- + H^+ \rightleftharpoons H_2O + Cl \quad (3)$$

$$Cl + Cl^- \rightleftharpoons Cl_2^- \quad (4)$$

$$2Cl_2^- \rightleftharpoons Cl_2 + 2Cl^- \quad (5)$$

where dissolved Cl_2 partitions to the gas phase. Reactions 1−5 have been invoked to explain field measurements of higher-than-expected daytime $Cl_{2(g)}$ production rates[7,10] and their correlation to aerosol nitrate concentration and aerosol surface area.[13] However, the mechanism by which $Cl_{2(g)}$ is formed remains uncertain,[27] and it is unclear if other active chlorine species are formed during this process.

We used laboratory experiments and kinetic modeling to explore the mechanism of nitrate photolysis in chloride solutions. A temperature-controlled (296 K) wetted-wall flow reactor (WWFR)[28] (Figure S4) was used to study the gas-phase products evolved when aqueous chloride solutions containing nitrate were photolyzed by UV light (300−375

Received: March 29, 2023
Published: July 18, 2023

https://doi.org/10.1021/jacs.3c03112
J. Am. Chem. Soc. 2023, 145, 15652−15657

nm). In a typical experiment, the inside surface of the WWFR was coated by a slowly flowing (0.05 cm s^{-1}) aqueous solution of $NaNO_3$ (0.1 M) and NaCl (1.0 M) at pH 4, creating a 75 μm thick water film that mimics the high surface-area-to-volume ratio of marine aqueous SSA.[29] Ultrapure air at 90% relative humidity was flowed over the aqueous layer to deliver gas-phase reactants and products to an iodide-based chemical ionization mass spectrometer (CIMS).[30,31] Experimental details are included in the Supporting Information. As shown in Figure 1, photolysis of 0.1 M NO_3^- in the presence of 1 M

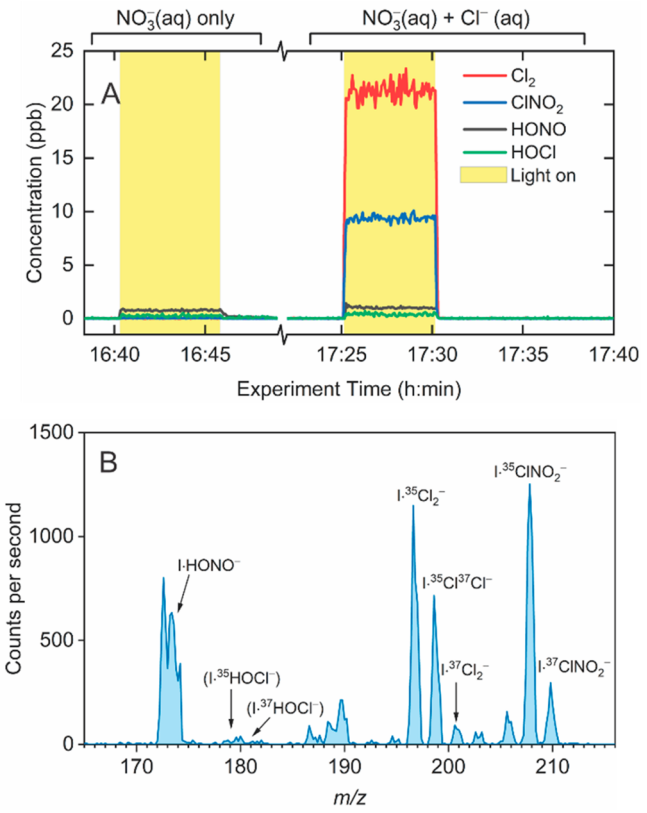

Figure 1. (A) Products formed when 0.1 M NO_3^- is photolyzed (300−320 nm) in the presence or absence of 1.0 M Cl^- (pH 4) in the WWFR. (B) Product verification using iodide ion chemical ionization mass spectrometry (CIMS).

Cl^- produces 21 ppb of Cl_2 and 9 ppb of $ClNO_2$, which are not products observed when NO_3^- is irradiated in the absence of Cl^-. Unambiguous identification of products was based on expected m/z values and isotope patterns derived from the mass spectra (Figure 1B). The appearance of Cl_2 is consistent with multiphase modeling studies[27,32,33] as well as a recent experimental and modeling study of NO_3^- photolysis in acidic chloride solutions.[13] However, different from previous studies, $ClNO_2$ and HOCl formation is demonstrated here for the first time.

A possible mechanism responsible for $ClNO_2$ formation starts with the pH-dependent equilibrium among Cl_2, HOCl, and Cl^- in aqueous solution (reaction 6). Formation of Cl_2 and HOCl is followed by reactions 7 and 8, which involve Cl^+ transfer to NO_2^-.[34]

$$Cl_2 + H_2O \rightleftharpoons HOCl + Cl^- + H^+ \quad (6)$$

$$Cl_2 + NO_2^- \rightarrow ClNO_2 + Cl^- \quad (7)$$

$$HOCl + NO_2^- \rightarrow ClNO_2 + OH^- \quad (8)$$

Reaction 6 is well-known chlorine−water chemistry,[35] and the mechanism of $ClNO_2$ formation from reactions 7 and 8 has been characterized previously in laboratory studies.[34,36,37]

The Cl_2/HOCl equivalence point of reaction 6 is at pH 3 for a 1 M Cl^- solution,[38] suggesting that HOCl should also be present under the conditions of our experiment, as well as under atmospheric conditions. When Cl_2 is formed, it rapidly partitions to the gas phase due to its low Henry's law coefficient.[39] The low yield of $HOCl_{(g)}$ and high yield of $ClNO_{2(g)}$ in Figure 1A suggest that residual $HOCl_{(g)}$ has reacted to near completion with NO_2^-/HONO. To test this, we measured gas-phase species originating from aqueous films composed of pH 6 solutions of 25 μM NO_2^- and/or 25 μM HOCl. As shown in Figure 2, a solution of NO_2^- emits

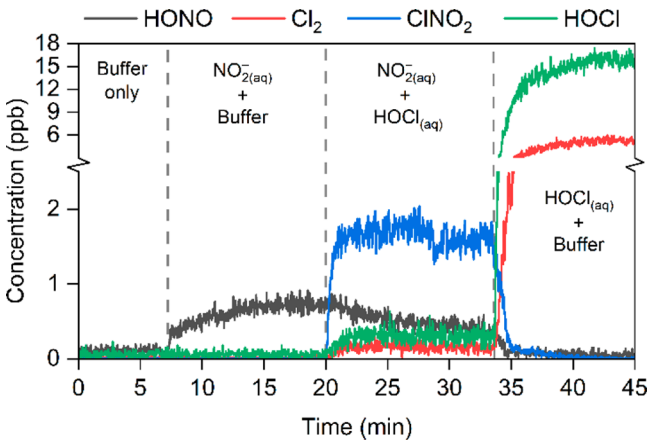

Figure 2. Gases evolved when solutions containing the indicated solutes are mixed prior to entering the WWFR. $ClNO_{2(g)}$ is generated as the major product when separate solutions of NO_2^- (50 μM) and HOCl (50 μM) are mixed (1:1 v/v) together. $HOCl_{(g)}$ and $Cl_{2(g)}$ are evolved from the HOCl solution only when the NO_2^- solution is replaced by a nitrite-free buffer solution. All solutions are buffered at pH 6 with 5 mM NaH_2PO_4.

$HONO_{(g)}$ while solutions of pure HOCl emit both $Cl_{2(g)}$ and $HOCl_{(g)}$, as expected. When the two solutions are mixed at the flow reactor inlet, the $HONO_{(g)}$ concentration decreases, while $ClNO_{2(g)}$ appears and ~150 ppt of $HOCl_{(g)}$ remains. These observations are consistent with previous studies,[34,36,37] supporting that HOCl and Cl_2 are precursors to $ClNO_2$ formation.

To assess whether this mechanism explains the observations, we compared the experimental results to the output of a kinetic model that includes established Cl-activation chemistry,[33] including reactions 1−8 leading to $ClNO_{2(g)}$ (see SI). Model predictions are compared to the average steady-state experimental concentrations of $ClNO_{2(g)}$, $Cl_{2(g)}$, $HOCl_{(g)}$, and $HONO_{(g)}$ in Figure 3. A model that includes NO_3^- photochemistry and standard chlorine activation via OH and nitrogen oxide chemistry (Model 1) underestimates the observed $Cl_{2(g)}$ by a factor of 4 at pH 4. Predicted $ClNO_2$ concentrations were low, since the amount of Cl_2 and HOCl available to react with NO_2^- was insufficient, suggesting that Model 1 is missing an additional source of Cl_2/HOCl.

An alternative mechanism not considered in current atmospheric chemistry models is the oxidation of Cl^- by $O(^3P)$, which is produced along with NO_2^- in reaction 1b.

https://doi.org/10.1021/jacs.3c03112
J. Am. Chem. Soc. 2023, 145, 15652−15657

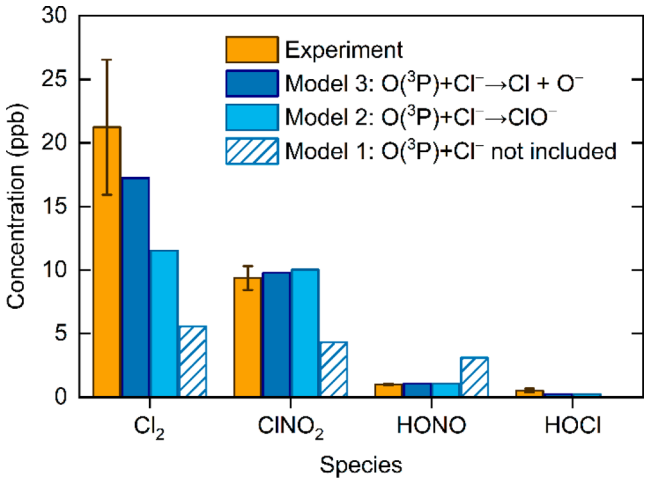

Figure 3. Comparisons of steady-state product concentrations determined from the WWFR experiment to concentrations predicted by three different kinetic models.

Amichai and Treinin[40] first studied this reaction by measuring its competitive kinetics relative to $O(^3P) + O_2$. Using their data, a second-order rate constant of $5.6(\pm4.2) \times 10^5$ M^{-1} s^{-1} can be derived, which is similar to value of $1.64(\pm0.01) \times 10^5$ M^{-1} s^{-1} reported more recently by Jirásek and Lukeš.[41] Although mechanistic studies are limited for this reaction,[41,42] two reaction channels with Cl^- are possible:

$$O(^3P) + Cl^- \rightarrow [O\cdots Cl^-] \rightarrow OCl^- \quad (9a)$$

$$\rightarrow O^- + Cl \quad (9b)$$

Reaction 9a is an addition reaction forming OCl^- and HOCl (pK_a = 7.5) directly, while reaction 9b involves an electron transfer to form a Cl atom, which would subsequently form Cl_2 and HOCl via reactions 2−6. Reactions 9a and 9b were added to Model 1 to determine if they provide the additional HOCl/Cl_2 required to match the experimental observations in Figure 1. As shown in Figure 3, inclusion of reaction 9a as Model 2 produces equal amounts of Cl_2 and HOCl, while inclusion of reaction 9b as Model 3 gives Cl_2 and $ClNO_2$ concentrations in a ratio of 1.8:1, in agreement with our observations. Thus, the experimental data support the electron-transfer reaction (9b) as the source of Cl_2/HOCl in the system, although work is underway to verify this. Model 3 suggests that 68% of $Cl_{2(g)}$ in the system comes from reaction 9b, while the remaining 32% comes from reactions 2−5.

To observe halide activation by $O(^3P)$ in the absence of reactive nitrogen, we used bromate (BrO_3^-) as the $O(^3P)$ source. Previous studies found that $O(^3P)$ is the major photoproduct from BrO_3^- photolysis, being favored over OH by a factor of 1.6.[40,43] For comparison, NO_3^- generates 2−10 times more OH than $O(^3P)$ at 300 nm.[24,25] Therefore, we expect secondary chemistry in irradiated BrO_3^- solutions to be dominated by $O(^3P)$ reactions. As shown in Figures 4A and B, photolysis of an air-saturated solution of 0.1 mM BrO_3^- at 254 nm generates 125 ppb of Cl_2, which is an order of magnitude higher than the amount of Cl_2 observed from NO_3^- under otherwise identical experimental conditions. The greater quantity of $Cl_{2(g)}$ formed during Cl^- oxidation in BrO_3^- solutions compared to the NO_3^- system is due to the faster photolysis rate of BrO_3^- and the absence of NO_2^-, which scavenges Cl_2 in the NO_3^- system. Although this experiment

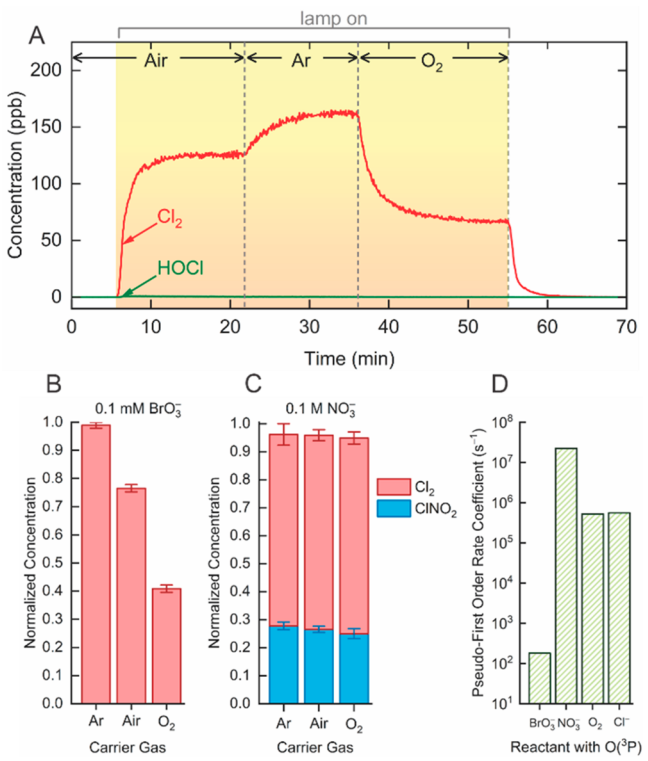

Figure 4. (A) Aqueous solution of BrO_3^- (0.1 mM) and Cl^- (1.0 M) at pH 4 saturated with 1 atm of air, argon, or O_2, irradiated at 254 nm. Relative concentrations of active chlorine species (normalized to maximum reached under anoxic conditions) formed in solutions shown in panel A (B) and NO_3^- solutions (0.1 M) and Cl^- (1.0 M) at pH 4 at λ = 300−320 nm (C). (D) Pseudo-first-order rate constant for the aqueous-phase reaction of $O(^3P)$ with BrO_3^- (0.1 mM), NO_3^- (0.1 M), O_2 (0.13 mM), or Cl^- (1.0 M).

suggests that the $O(^3P)$ plays a role in Cl_2 formation during BrO_3^- photolysis, it is still possible that some of the Cl_2 observed originates from Cl^- oxidation by the OH radical, which is the minor BrO_3^- photoproduct.

To distinguish between Cl^- oxidation via $O(^3P)$ and OH in the BrO_3^- system, we used dissolved oxygen as a scavenger of $O(^3P)$. OH is unreactive toward O_2, while $O(^3P)$ reacts with O_2 with a second-order rate constant of 4×10^9 M^{-1} s^{-1};[44] thus, chemistry under anoxic conditions should favor products originating from $O(^3P)$ reactions. As shown in Figures 4A and B, when BrO_3^- + Cl^- solutions are photolyzed under anoxic conditions (sparged with Ar), the amount of Cl_2 formed increases by 29% compared to solutions irradiated in air. Furthermore, when the solution is reoxygenated and irradiated in the presence of 1 atm of O_2, the yield of Cl_2 drops by 59% relative to levels achieved under anoxic conditions. The sensitivity of Cl_2 formation toward dissolved O_2 concentrations is strong evidence that $O(^3P)$ oxidizes chloride.

Next, we assessed whether Cl_2 and $ClNO_2$ production in the NO_3^- system is sensitive to dissolved O_2. At concentrations of 0.1 M NO_3^- and 1 M Cl^- (pH 4), the amounts of Cl_2 and $ClNO_2$ formed were invariant regardless of whether the solution was sparged with Ar, air, or pure O_2 (Figure 4C). This is explained by the superior effectiveness of NO_3^- as a scavenger for $O(^3P)$ vs O_2 and BrO_3^-. Considering published second-order rate constants[40] and aqueous concentrations of BrO_3^-, NO_3^-, Cl^-, and O_2[45] under air-saturated conditions, the NO_3^- + $O(^3P)$ reaction is 5 orders of magnitude faster

https://doi.org/10.1021/jacs.3c03112
J. Am. Chem. Soc. 2023, 145, 15652−15657

than BrO_3^- + $O(^3P)$, and ~20 times faster than O_2 + $O(^3P)$ (Figure 4D).

The importance of this mechanism as a source of reactive chlorine gases in the atmosphere depends on the chemical composition of the condensed phase. Atmospheric aerosols contain organic components and transition metals that may scavenge reactive species such as $O(^3P)$, dichloride radial anion (Cl_2^-), or Cl atoms,[27] thereby influencing the overall effectiveness and outcome of the aqueous-phase chemistry described here. Moreover, differences in aerosol particle vs cloud chemistry are expected as the aqueous-phase concentrations of organic compounds in cloud water are lower compared to wet aerosol particles.

To investigate the conditions under which $O(^3P)$ chemistry will have an impact on chlorine activation in aerosols, we ran several simulations over a range of Cl^- and dissolved organic matter (DOM) concentrations[2,15,46,47] (see SI section 2.2). There is a paucity of rate constants for the reaction of $O(^3P)$ with organic molecules in the aqueous phase. However, a comparison of gas-phase rate constants for the reaction of $O(^3P)$ with organic molecules in the gas phase suggests that $O(^3P)$ reacts an order of magnitude slower than comparable OH radical reactions.[48−50] Assuming a typical aqueous-phase OH reaction rate constant of ~10^9 M^{-1} s^{-1} for organic matter,[51] we set the aqueous-phase $O(^3P)$ + DOM reaction rate constant to be 10^8 M^{-1} s^{-1}. The NO_3^- concentration was held at 0.1 M, while the concentrations of Cl^- and DOM were varied between 0.01 and 1 M, and between 0.001 and 0.1 M, respectively (Table S3). Dissolved O_2 concentrations were calculated based on the ionic strength-dependent Henry's law constant.[45]

Model results indicate that chloride is the most important sink for $O(^3P)$ when Cl^- concentrations are highest and DOM content is lowest. At lower chloride concentrations, dissolved O_2 and DOM are the most important sinks for $O(^3P)$, with the latter taking over as the major sink for high organic content aerosol. We conclude that this mechanism is most important for nitrate-containing particles with high Cl^- and low DOM concentrations such as in the case for saturated salt solutions that may be present in SSA at their deliquescence point, or for phase-separated aerosols containing distinct domains of organic components and salts.[52] Such conditions could be found in the polluted marine boundary layer, near salt lakes, and in continental regions where high Cl^- levels in aerosols have been observed.[5,30,53]

Formation of $ClNO_{2(g)}$ from nitrate photolysis has important implications for atmospheric chemistry due to its relatively short photochemical lifetime of $ClNO_2$ during the daytime (5 min at noontime),[54] which makes $ClNO_2$ a strong daytime source of gas-phase Cl atoms. Most atmospheric gases react more rapidly with the Cl atom than with the OH radical. Thus, Cl activation in nitrate-containing SSA can initiate photooxidation chemistry that impacts the lifetime of trace gases and leads to O_3 formation, especially in the MBL and in coastal regions when marine and polluted continental air masses mix. The described $O(^3P)$ chemistry should be included in chemical models of all scales to better understand oxidative multiphase chemistry and halogen cycling.

■ ASSOCIATED CONTENT

Supporting Information

The Supporting Information is available free of charge at https://pubs.acs.org/doi/10.1021/jacs.3c03112.

Experimental Methods section and description of the kinetics model used to study the mechanism of chlorine activation (PDF)

■ AUTHOR INFORMATION

Corresponding Author

Jonathan D. Raff − *Paul H. O'Neill School of Public & Environmental Affairs and Department of Chemistry, Indiana University, Bloomington, Indiana 47405, United States;* orcid.org/0000-0002-2574-8061; Email: jdraff@indiana.edu

Authors

Evan Z. Dalton − *Department of Chemistry, Indiana University, Bloomington, Indiana 47405, United States;* orcid.org/0000-0002-4900-3902

Erik H. Hoffmann − *Atmospheric Chemistry Department, Leibniz Institute for Tropospheric Research, 04318 Leipzig, Germany;* orcid.org/0000-0003-4560-0125

Thomas Schaefer − *Atmospheric Chemistry Department, Leibniz Institute for Tropospheric Research, 04318 Leipzig, Germany;* orcid.org/0000-0001-7995-4285

Andreas Tilgner − *Atmospheric Chemistry Department, Leibniz Institute for Tropospheric Research, 04318 Leipzig, Germany;* orcid.org/0000-0003-4021-4874

Hartmut Herrmann − *Atmospheric Chemistry Department, Leibniz Institute for Tropospheric Research, 04318 Leipzig, Germany;* orcid.org/0000-0001-7044-2101

Complete contact information is available at: https://pubs.acs.org/10.1021/jacs.3c03112

Notes

The authors declare no competing financial interest.

■ ACKNOWLEDGMENTS

We thank Dave Tanner for his indispensable advice with CIMS operation and repairs. We also thank Dr. Christian George for helpful discussions. Financial support for this study came from the National Science Foundation (Awards AGS-1352375 and CHE-2305078), NSF Graduate Research Fellowship to E.Z.D. (Award 2019286041), Indiana Space Grant Consortium Fellowship to E.Z.D., U.S. Department of Energy's Office of Biological and Environmental Research (BER) Environmental System Science (ESS) Program (Award DE-SC0014443). We are grateful to the Breathing Nature Initiative at the University of Leipzig for supporting collaborative work between TROPOS and Indiana University.

■ REFERENCES

(1) Barrie, L. A.; Bottenheim, J. W.; Schnell, R. C.; Crutzen, P. J.; Rasmussen, R. A. Ozone destruction and photochemical reactions at polar sunrise in the lower Arctic atmosphere. *Nature* **1988**, *334*, 138−141.

(2) Vogt, R.; Crutzen, P. J.; Sander, R. A mechanism for halogen release from sea-salt aerosol in the remote marine boundary layer. *Nature* **1996**, *383*, 327−330.

(3) Foster, K. L.; Plastridge, R. A.; Bottenheim, J. W.; Shepson, P. B.; Finlayson-Pitts, B. J.; Spicer, C. W. The role of Br_2 and BrCl in surface ozone destruction at polar sunrise. *Science* **2001**, *291*, 471−474.

(4) Wang, X.; Jacob, D. J.; Downs, W.; Zhai, S.; Zhu, L.; Shah, V.; Holmes, C. D.; Sherwen, T.; Alexander, B.; Evans, M. J.; Eastham, S. D.; Neuman, J. A.; Veres, P. R.; Koenig, T. K.; Volkamer, R.; Huey, L. G.; Bannan, T. J.; Percival, C. J.; Lee, B. H.; Thornton, J. A. Global

tropospheric halogen (Cl, Br, I) chemistry and its impact on oxidants. *Atmos. Chem. Phys.* **2021**, *21*, 13973−13996.
(5) Osthoff, H. D.; Roberts, J. M.; Ravishankara, A. R.; Williams, E. J.; Lerner, B. M.; Sommariva, R.; Bates, T. S.; Coffman, D.; Quinn, P. K.; Dibb, J. E.; Stark, H.; Burkholder, J. B.; Talukdar, R. K.; Meagher, J.; Fehsenfeld, F. C.; Brown, S. S. High levels of nitryl chloride in the polluted subtropical marine boundary layer. *Nat. Geosci.* **2008**, *1*, 324−328.
(6) Roberts, J. M.; Osthoff, H. D.; Brown, S. S.; Ravishankara, A. R. N_2O_5 oxidizes chloride to Cl_2 in acidic atmospheric aerosol. *Science* **2008**, *321*, 1059−1059.
(7) Oum, K. W.; Lakin, M. J.; DeHaan, D. O.; Brauers, T.; Finlayson-Pitts, B. J. Formation of Molecular Chlorine from the Photolysis of Ozone and Aqueous Sea-Salt Particles. *Science* **1998**, *279*, 74−76.
(8) Knipping, E. M.; Lakin, M. J.; Foster, K. L.; Jungwirth, P.; Tobias, D. J.; Gerber, R. B.; Dabdub, D.; Finlayson-Pitts, B. J. Experiments and simulations of ion-enhanced interfacial chemistry on aqueous NaCl aerosols. *Science* **2000**, *288*, 301−306.
(9) Finlayson-Pitts, B. J.; Ezell, M. J.; Pitts, J. N. Formation of chemically active chlorine compounds by reactions of atmospheric NaCl particles with gaseous N_2O_5 and $ClONO_2$. *Nature* **1989**, *337*, 241−244.
(10) Spicer, C. W.; Chapman, E. G.; Finlayson-Pitts, B. J.; Plastridge, R. A.; Hubbe, J. M.; Fast, J. D.; Berkowitz, C. M. Unexpectedly high concentrations of molecular chlorine in coastal air. *Nature* **1998**, *394*, 353−356.
(11) Lawler, M. J.; Sander, R.; Carpenter, L. J.; Lee, J. D.; von Glasow, R.; Sommariva, R.; Saltzman, E. S. HOCl and Cl_2 observations in marine air. *Atmos. Chem. Phys.* **2011**, *11*, 7617−7628.
(12) Wang, X.; Jacob, D. J.; Eastham, S. D.; Sulprizio, M. P.; Zhu, L.; Chen, Q.; Alexander, B.; Sherwen, T.; Evans, M. J.; Lee, B. H.; Haskins, J. D.; Lopez-Hilfiker, F. D.; Thornton, J. A.; Huey, G. L.; Liao, H. The role of chlorine in global tropospheric chemistry. *Atmos. Chem. Phys.* **2019**, *19*, 3981−4003.
(13) Peng, X.; Wang, T.; Wang, W.; Ravishankara, A. R.; George, C.; Xia, M.; Cai, M.; Li, Q.; Salvador, C. M.; Lau, C.; Lyu, X.; Poon, C. N.; Mellouki, A.; Mu, Y.; Hallquist, M.; Saiz-Lopez, A.; Guo, H.; Herrmann, H.; Yu, C.; Dai, J.; Wang, Y.; Wang, X.; Yu, A.; Leung, K.; Lee, S.; Chen, J. Photodissociation of particulate nitrate as a source of daytime tropospheric Cl_2. *Nature Comm.* **2022**, *13*, 939.
(14) Chen, Q.; Xia, M.; Peng, X.; Yu, C.; Sun, P.; Li, Y.; Liu, Y.; Xu, Z.; Xu, Z.; Wu, R.; Nie, W.; Ding, A.; Zhao, Y.; Wang, T. Large Daytime Molecular Chlorine Missing Source at a Suburban Site in East China. *J. Geophys. Res.-Atmos.* **2022**, *127*, e2021JD035796.
(15) Anastasio, C.; Newberg, J. T. Sources and sinks of hydroxyl radical in sea-salt particles. *J. Geophys. Res.-Atmos.* **2007**, *112*, D10306.
(16) Gori, E. G.; Petriconi, G. L.; Papee, H. M. Ultraviolet Photolysis of Sodium Nitrate Solutions in the Laboratory and by Sunlight. *Nature* **1968**, *217*, 248−249.
(17) Wingen, L. M.; Moskun, A. C.; Johnson, S. N.; Thomas, J. L.; Roeselova, M.; Tobias, D. J.; Kleinman, M. T.; Finlayson-Pitts, B. J. Enhanced surface photochemistry in chloride-nitrate ion mixtures. *Phys. Chem. Chem. Phys.* **2008**, *10*, 5668−5677.
(18) George, I. J.; Anastasio, C. Release of gaseous bromine from the photolysis of nitrate and hydrogen peroxide in simulated sea-salt solutions. *Atmos. Environ.* **2007**, *41*, 543−553.
(19) Abbatt, J.; Oldridge, N.; Symington, A.; Chukalovskiy, V.; McWhinney, R. D.; Sjostedt, S.; Cox, R. A. Release of Gas-Phase Halogens by Photolytic Generation of OH in Frozen Halide−Nitrate Solutions: An Active Halogen Formation Mechanism? *J. Phys. Chem. A* **2010**, *114*, 6527−6533.
(20) Richards, N. K.; Wingen, L. M.; Callahan, K. M.; Nishino, N.; Kleinman, M. T.; Tobias, D. J.; Finlayson-Pitts, B. J. Nitrate ion photolysis in thin water films in the presence of bromide ions. *J. Phys. Chem. A* **2011**, *115*, 5810−5821.
(21) Richards, N. K.; Finlayson-Pitts, B. J. Production of Gas Phase NO_2 and Halogens from the Photochemical Oxidation of Aqueous Mixtures of Sea Salt and Nitrate Ions at Room Temperature. *Environ. Sci. Technol.* **2012**, *46*, 10447−10454.
(22) Mack, J.; Bolton, J. R. Photochemistry of Nitrite and Nitrate in Aqueous Solution: A Review. *J. Photochem. Photobiol., A* **1999**, *128*, 1−13.
(23) Zellner, R.; Exner, M.; Herrmann, H. Absolute OH quantum yields in the laser photolysis of nitrate, nitrite and dissolved H_2O_2 at 308 and 351 nm in the temperature range 278−353 K. *J. Atmos. Chem.* **1990**, *10*, 411−425.
(24) Benedict, K. B.; McFall, A. S.; Anastasio, C. Quantum Yield of Nitrite from the Photolysis of Aqueous Nitrate above 300 nm. *Environ. Sci. Technol.* **2017**, *51*, 4387−4395.
(25) Herrmann, H. On the photolysis of simple anions and neutral molecules as sources of O^-/OH, SO_x^- and Cl in aqueous solution. *Phys. Chem. Chem. Phys.* **2007**, *9*, 3935−3964.
(26) Yu, X.-Y.; Barker, J. R. Hydrogen Peroxide Photolysis in Acidic Aqueous Solutions Containing Chloride Ions. I. Chemical Mechanism. *J. Phys. Chem. A* **2003**, *107*, 1313−1324.
(27) Brauer, P.; Tilgner, A.; Wolke, R.; Herrmann, H. Mechanism development and modelling of tropospheric multiphase halogen chemistry: The CAPRAM Halogen Module 2.0 (HM2). *J. Atmos. Chem.* **2013**, *70*, 19−52.
(28) Utter, R. G.; Burkholder, J. B.; Howard, C. J.; Ravishankara, A. R. Measurement of the mass accommodation coefficient of ozone on aqueous surfaces. *J. Phys. Chem. A* **1992**, *96*, 4973−4979.
(29) Danckwerts, P. V. *Gas-Liquid Reactions*; McGraw-Hill Book Co., 1970.
(30) Mielke, L. H.; Furgeson, A.; Osthoff, H. D. Observation of $ClNO_2$ in a Mid-Continental Urban Environment. *Environ. Sci. Technol.* **2011**, *45*, 8889−8896.
(31) McNamara, S. M.; Chen, Q.; Edebeli, J.; Kulju, K. D.; Mumpfield, J.; Fuentes, J. D.; Bertman, S. B.; Pratt, K. A. Observation of N_2O_5 Deposition and $ClNO_2$ Production on the Saline Snowpack. *ACS Earth Space Chem.* **2021**, *5*, 1020−1031.
(32) Herrmann, H.; Majdik, Z.; Ervens, B.; Weise, D. Halogen production from aqueous tropospheric particles. *Chemosphere* **2003**, *52*, 485−502.
(33) Hoffmann, E. H.; Schrodner, R.; Tilgner, A.; Wolke, R.; Herrmann, H. CAPRAM reduction towards an operational multiphase halogen and dimethyl sulfide chemistry treatment in the chemistry transport model COSMO-MUSCAT(5.04e). *Geosci. Model. Dev.* **2020**, *13*, 2587−2609.
(34) Johnson, D. W.; Margerum, D. W. Non-metal redox kinetics: a reexamination of the mechanism of the reaction between hypochlorite and nitrite ions. *Inorg. Chem.* **1991**, *30*, 4845−4851.
(35) Wang, T. X.; Margerum, D. W. Kinetics of Reversible Chlorine Hydrolysis: Temperature Dependence and General-Acid/Base-Assisted Mechanisms. *Inorg. Chem.* **1994**, *33*, 1050−1055.
(36) Frenzel, A.; Scheer, V.; Sikorski, R.; George, C.; Behnke, W.; Zetzsch, C. Heterogeneous Interconversion Reactions of $BrNO_2$, $ClNO_2$, Br_2, and Cl_2. *J. Phys. Chem. A* **1998**, *102*, 1329−1337.
(37) Thaler, R. D.; Mielke, L. H.; Osthoff, H. D. Quantification of Nitryl Chloride at Part Per Trillion Mixing Ratios by Thermal Dissociation Cavity Ring-Down Spectroscopy. *Anal. Chem.* **2011**, *83*, 2761−2766.
(38) Cherney, D. P.; Duirk, S. E.; Tarr, J. C.; Collette, T. W. Monitoring the speciation of aqueous free chlorine from pH 1 to 12 with Raman spectroscopy to determine the identity of the potent low-pH oxidant. *Appl. Spectrosc.* **2006**, *60*, 764−772.
(39) Sander, S. P.; Finlayson-Pitts, B. J.; Friedl, R. R.; Golden, D. M.; Huie, R. E.; Keller-Rudek, H.; Kolb, C. E.; Kurylo, M. J.; Molina, M. J.; Moortgat, G. K.; Orkin, V. L.; Ravishankara, A. R.; Wine, P. H. *Chemical Kinetics and Photochemical Data for Use in Atmospheric Studies*, Evaluation Number 15, JPL Publication 06-2; Jet Propulsion Laboratory, 2006.
(40) Amichai, O.; Treinin, A. Chemical Reactivity of $O(^3P)$ Atoms in Aqueous Solution. *Chem. Phys. Lett.* **1969**, *3*, 611−613.

https://doi.org/10.1021/jacs.3c03112
J. Am. Chem. Soc. 2023, 145, 15652−15657

(41) Jirásek, V.; Lukeš, P. Competitive reactions in Cl^- solutions treated by plasma-supplied O atoms. *J. Phys. D: Appl. Phys.* **2020**, *53*, 505206.
(42) Wende, K.; Williams, P.; Dalluge, J.; Van Gaens, W.; Aboubakr, H.; Bischof, J.; von Woedtke, T.; Goyal, S. M.; Weltmann, K.-D.; Bogaerts, A.; Masur, K.; Bruggeman, P. J. Identification of the biologically active liquid chemistry induced by a nonthermal atmospheric pressure plasma jet. *Biointerphases* **2015**, *10*, 029518.
(43) Brown, W. G.; Hart, E. J. Effect of pH on oxygen(^{3}P) atom formation in.gamma.-ray irradiated aqueous solutions. *J. Phys. Chem. A* **1978**, *82*, 2539−2542.
(44) Kläning, U. K.; Sehested, K.; Wolff, T. Ozone formation in laser flash photolysis of oxoacids and oxoanions of chlorine and bromine. *J. Chem. Soc., Faraday Trans. 1* **1984**, *80*, 2969−2979.
(45) Schumpe, A.; Adler, I.; Deckwer, W.-D. Solubility of oxygen in electrolyte solutions. *Biotechnol. Bioeng.* **1978**, *20*, 145−150.
(46) Straub, D. J.; Lee, T.; Collett, J. L., Jr Chemical composition of marine stratocumulus clouds over the eastern Pacific Ocean. *J. Geophys. Res.-Atmos.* **2007**, *112*, D04307.
(47) van Pinxteren, D.; Fomba, K. W.; Mertes, S.; Müller, K.; Spindler, G.; Schneider, J.; Lee, T.; Collett, J. L.; Herrmann, H. Cloud water composition during HCCT-2010: Scavenging efficiencies, solute concentrations, and droplet size dependence of inorganic ions and dissolved organic carbon. *Atmos. Chem. Phys.* **2016**, *16*, 3185−3205.
(48) Calvert, J. G.; Becker, K. H.; Kamens, R. M.; Seinfeld, J. H.; Wallington, T. H.; Yarwood, G. *The Mechanisms of Atmospheric Oxidation of the Aromatic Hydrocarbons*; Oxford University Press, 2002.
(49) Cvetanović, R. J. Evaluated Chemical Kinetic Data for the Reactions of Atomic Oxygen O(^{3}P) with Unsaturated Hydrocarbons. *J. Phys. Chem. Ref. Data* **1987**, *16*, 261−326.
(50) Herron, J. T. Evaluated Chemical Kinetic Data for the Reactions of Atomic Oxygen O(^{3}P) with Saturated Organic Compounds in the Gas Phase. *J. Phys. Chem. Ref. Data* **1988**, *17*, 967−1026.
(51) Appiani, E.; Page, S. E.; McNeill, K. On the Use of Hydroxyl Radical Kinetics to Assess the Number-Average Molecular Weight of Dissolved Organic Matter. *Environ. Sci. Technol.* **2014**, *48*, 11794−11802.
(52) Bondy, A. L.; Bonanno, D.; Moffet, R. C.; Wang, B.; Laskin, A.; Ault, A. P. The diverse chemical mixing state of aerosol particles in the southeastern United States. *Atmos. Chem. Phys.* **2018**, *18*, 12595−12612.
(53) McNamara, S. M.; Kolesar, K. R.; Wang, S.; Kirpes, R. M.; May, N. W.; Gunsch, M. J.; Cook, R. D.; Fuentes, J. D.; Hornbrook, R. S.; Apel, E. C.; China, S.; Laskin, A.; Pratt, K. A. Observation of Road Salt Aerosol Driving Inland Wintertime Atmospheric Chlorine Chemistry. *ACS Central Science* **2020**, *6*, 684−694.
(54) Raff, J. D.; Njegic, B.; Chang, W.; Gordon, M. S.; Dabdub, D.; Gerber, B.; Finlayson-Pitts, B. J. Surface-mediated reactions of nitrogen oxides with hydrogen chloride: Indoor and outdoor chlorine activation. *Proc. Natl. Acad. Sci. U.S.A.* **2009**, *106*, 13647−13654.

https://doi.org/10.1021/jacs.3c03112
J. Am. Chem. Soc. 2023, 145, 15652−15657